Sporophytic control of pollen meiotic progression is mediated by tapetum expression of AMS

Alison C Tidy[1,7], Ivana Ferjentsikova[1,7], Gema Vizcay-Barrena[1], Bing Liu[2], Wenzhe Yin[1], James D Higgins[3], Xu Jie[4], Dabing Zhang[4,5], Danny Geelen[6], Zoe A Wilson[1]*

[1] Division of Plant & Crop Sciences, School of Biosciences, University of Nottingham, Sutton Bonington Campus, Loughborough, Leics., LE12 5RD, UK

[2] College of Life Sciences, South-Central University for Nationalities, 430074 Wuhan, China

[3] Department of Genetics and Genome Biology, University of Leicester, University Road, Leicester, LE1 7RH, UK

[4] Joint International Research Laboratory of Metabolic & Developmental Sciences, School of Life Sciences and Biotechnology, Shanghai Jiao Tong University, Shanghai 200240, China

[5] School of Agriculture, Food and Wine, University of Adelaide, Waite Campus, Urrbrae, South Australia 5064, Australia

[6] Department of Plant Production, Ghent University, Coupure Links 653, geb. A, 9000 Gent, Belgium

[7] Co-first author

* Corresponding Author: Zoe A Wilson

Email: zoe.wilson@nottingham.ac.uk

ONE SENTENCE SUMMARY: *AMS* is key to tapetum-meiocyte crosstalk by enabling late meiosis progression, cytokinesis, RMA organisation and callose deposition.

ABSTRACT

Pollen development has dependency on the tapetum, a sporophytic anther cell layer surrounding the microspores, which functions in pollen wall formation, but is also essential for meiosis-associated development. There is clear evidence of crosstalk and co-regulation between the tapetum and microspores, however how this is achieved is currently not characterised. *ABORTED MICROSPORES (AMS)*, a tapetum transcription factor, is important for pollen wall formation, but also has an undefined role in early pollen development. We conducted a detailed investigation of chromosome behaviour, cytokinesis, radial microtubule array (RMA) organisation and callose formation in the *ams* mutant. Early meiosis initiates normally in *ams*, shows delayed progression after the pachytene stage, and then fails during late meiosis, with disorganised RMA, defective cytokinesis, abnormal callose formation and microspore degeneration, alongside abnormal tapetum development. Here, we show that selected meiosis-associated genes are directly repressed by AMS, and that AMS is essential for late meiosis progression. Our findings indicate that AMS has a dual function in tapetum-meiocyte crosstalk by playing an important regulatory role during late meiosis, in addition to its previously characterised role in pollen wall formation. AMS is critical for RMA organisation, callose deposition and therefore cytokinesis and is involved in the crosstalk between the gametophyte and sporophytic tissues, which enables synchronous development of tapetum and microspores.

Key words: Pollen development, anther, male sterile, tapetum, meiosis, AMS, *ABORTED MICROSPORES*, radial microtubule array, cytokinesis**,** callose

INTRODUCTION

The tapetum is one of the most important cell layers in the anther. It is in direct contact with the developing pollen and plays an uncharacterised regulatory role in meiosis, and is essential for the subsequent biosynthesis and control of pollen wall formation (Zhang and Yang 2014). Tapetum cell differentiation coincides with anther meiotic development, with the tapetum providing a major secretory function in pollen wall formation and pollen maturation by providing enzymes for microspore release from tetrads, sporopollenin biosynthesis and secretion of pollen wall components (Liu and Fan 2013; Shi et al. 2015; Wang et al. 2018). Meiosis occurs in Arabidopsis stage 6 anthers and several meiotic regulators involved in pollen development have been identified (Sanders et al. 1999; Chang et al. 2011; Caryl et al. 2003; Liu and Qu 2008).

Although the tapetum is critical in supporting pollen development following the completion of meiosis, there has been uncertainty regarding its precise role in meiosis. A number of mutants lacking a differentiated tapetum cell layer, such as *excess microsporocytes1* (*ems1*) and *tapetum determinant1* (*tpd1*), indicate that a functional tapetum is required for the completion of meiosis (Zhao et al. 2002), but the initiation of meiosis in these mutants occurs apparently normally. The control of tapetum development has been shown to be tightly regulated, with rapid turnover of specific proteins and feed-forward and feed-back regulatory loops. These are controlled by key tapetum-expressed transcriptional factors such as *DYSFUNCTIONAL TAPETUM1 (DYT1), DEFECTIVE IN TAPETAL DEVELOPMENT (TDF1), ABORTED MICROSPORE (AMS), MALE STERILE 188 (MS188/MYB80/MYB103)*, and *MALE STERILE 1 (MS1)* which are part of a regulatory cascade directing pollen development (Cui et al. 2016; Fu et al. 2014; Xiong et al. 2016; Wang et al. 2018). The *ams, dyt1* and *tdf1* mutants are defective in tapetum function around the time of meiosis and therefore they are potential key players regulating transcription associated with meiotic stages in male microspores. These mutants show tapetum hypertrophy and microsporocyte degeneration (Zhang et al. 2006; Sorensen et al. 2003), this tapetum phenotype differs from other tapetum male sterile mutants that are later in the developmental progression such as *ms188/myb80* and *ms1* which produce single microspores, which then degenerate (Yang et al. 2007; Zhang et al. 2007; Xu et al. 2014).

AMS encodes for a basic helix-loop-helix (bHLH) protein that is expressed specifically in the tapetum; it shows biphasic protein expression starting at anther stage 5-6 (pre-meiotically), declining and then increasing from the free microspore to bicellular pollen stages (stage 8-11) (Ferguson et al.

2017). *MS188/MYB80* is a direct downstream target of AMS and both have established roles in sporopollenin formation (Cui et al. 2016; Fu et al. 2014; Xiong et al. 2016); extensive gene expression changes (549 genes) are observed in the *ams* mutant, including direct regulation of 23 genes involved in sporopollenin biosynthesis and secretion (Xu et al. 2010; Xu et al. 2014). This late role of AMS in pollen wall formation is well established, however we have shown that functional AMS protein is also required during early pollen development (Ferguson et al. 2017). Here we have investigated this early role of AMS during meiosis and tetrad formation and have shown that AMS is critical for Radial Microtubule Array (RMA) organisation, callose deposition and cytokinesis to allow correct tetrad formation, alongside its established subsequent role later in pollen wall development.

MATERIALS AND METHODS

Plant materials and growth conditions

Arabidopsis thaliana (L.) Columbia-0 (Col-0) were used as wild-type; the mutants and transgenic lines used were SALK T-DNA line *ams* (Sorensen et al. 2003); ethyl methane sulfonate (EMS) mutant *tdf1* (Zhu et al. 2008), transposon tagged lines *dyt1-3*, *ms188-3*, *ms1-8* (Zhu et al. 2011), and inducible line AMSprom:AMS-GR-YFP in Col-0 background (Ferguson et al. 2017). Lines were grown according to Ferguson et al. (2017).

Cytology and microscope analysis

Fixation and preparation of slides for basic cytology was as described by Higgins et al. (2014). Terminal inflorescences were fixed in 3:1 ethanol:glacial acetic acid (EAA) overnight and then stored at -20°C. Fixed flower buds from a single inflorescence were separated to remove the post-meiosis buds for meiotic analysis, or collected based upon size range for stage analysis. Anthers were carefully isolated prior to enzymatic digestion. Buds were washed twice in 10mM citrate buffer pH 4.5 at room temperature (RT), then incubated in citrate buffer containing 0.3% w/v cytohelicase (C1794), 0.3% (w/v) pectolyase (C8274) and 0.3% (w/v) cellulase (P5936) (Sigma) for 30 min- 1h in a humid chamber at 37°C. Replacing the enzyme mixture with ice-cold citrate buffer stopped the reaction.

Meiotic progression was determined by staining pollen mother cells (PMC) from isolated anthers using 1µg/µL 4’,6-diamidino-2-phenylindole (DAPI; Sigma) in Vectashield (Vector Laboratories) anti-fade mounting medium after squashing and UV observation. Over 300 meiotic cells were imaged to follow meiotic progression. TEM samples were treated as described by Xu et al. (2010) and analysed according to Chen et al. (2011a). Callose staining was performed by releasing meiotic cells

in a drop of aniline blue solution (0.1% in 0.033% K_3PO_4). Over 200 meiotic cells were observed by callose staining. Semi-thin sections (0.5µm) were stained with alkalinised 1% toluidine blue.

5-ethynyl-2'-deoxyuridine (EdU) labelling for meiotic progression

Wild-type and *ams* flowering stems were cut under water and quickly transferred to 1mM EdU solution for 2h for uptake by their transpiration stream and incorporation into cells in S-phase. Stems were then removed, ends rinsed and placed into distilled water for the time course analysis. Whole inflorescences were fixed and prepared for cytology as described previously. Digested anthers were placed in 10 µl 60% (v/v) acetic acid, re-fixed in cold 3:1 EAA fixative, then slides dried. Meiosis progression was detected using Click-IT® EdU Alexa Fluor® 488 imaging (from step 4.1 of ClickIT® kit protocol; ThermoFisher Scientific). Slides were mounted in Vectashield and observed (488nm). Three biological replicates were performed, and 6 digested anthers were analysed per slide. Over 400 meiotic cells were imaged as part of this time course and the latest stage of development seen per time point was used to mark meiotic progression.

α-tubulin immunolocalisation

α-tubulin immunolocalisation was performed according to De Storme et al. (2012) with minor modifications. Inflorescences were treated with m-maleimidobenzoyl N-hydrosuccinimide ester (100mM in 50mM potassium phosphate buffer and 0.05% Triton X-100, pH 8; 30min under vacuum) and fixed in 4% paraformaldehyde, then washed in 50mM potassium phosphate buffer (pH 8) and digested as above for 90 min. After the first digestion, anthers were dissected, squashed, and fixed on a slide by freezing in liquid nitrogen. Released cells on the slide were then immobilized with a thin layer of 1% gelatine, 1% agarose, and 2.5% glucose, and digested again for 90min at 37°C. After rinsing with potassium phosphate buffer, immobilized cells were then incubated overnight at RT with rat α-tubulin primary antibody (0.3%; clone B-5-1-2; Sigma-Aldrich) in PBS 0.1% Triton X-100, and 4.5gL^{-1} BSA. Cells were rinsed three times with PBS and incubated for 5h with 0.5% secondary antibody (labelled goat anti-rat) at 37°C in the dark. After three PBS rinses, 40 µl of DAPI (2mg mL^{-1}) in Vectashield mounting medium was added to each slide and observed using a fluorescent microscope. Over 150 meiotic cells were imaged for spindle and RMA formation.

Immunolocalisation of meiotic proteins

Following the fixation steps meiocytes were squashed and immobilised on slides based on the protocol by Higgins et al. (2014). They were digested for 30 min at 37°C in the digestion medium, and subsequently incubated for 1 hour in PBS 1% Triton at RT. After 2 rinses with PBS 0.1% Triton, slides were incubated overnight at 4°C in primary antibodies (rabbit anti-ZYP1, rabbit anti-ASY1,

rabbit anti-SUN2 (kindly provided by Profs D.E. Evans and K. Graumann; (Armstrong et al. 2002; Higgins et al. 2005)) diluted at 1/100-1/300 in PBS, 1% BSA, then washed in PBS, 0.1% Triton 5 times for 10 min. After 2h incubation at 37°C with the secondary antibodies in PBS 1% BSA, slides were washed in PBS 0.1% Triton 5 times for 10 min and mounted in Vectashield antifade medium (Vector Laboratories) with 80 µg/ml propidium iodide. Over 50 meiotic cells were imaged with the different antibodies.

Expression analysis

Closed buds from inflorescences of control (Col-0), *ams*, AMS:AMS-GR-YFP in the wild-type Col-0 background were collected. AMSprom:AMS-GR-YFP transgenic lines and controls were dipped into 25µM dexamethasone (DEX) + 0.02% Silwet L-77 and left for 24h before collection. Total RNA was extracted from inflorescences (~100mg) (RNeasy Plant Kit, Qiagen). First-strand cDNAs were synthesized from 5µg total RNA using Superscript III reverse transcriptase (Invitrogen) and an oligo (dT) primer (Invitrogen). qRT-PCR analyses were performed using the Light Cycler 480 real-time PCR system (Roche Applied Science), using Brilliant SYBR Green QPCR Master Mix (Fermentas). At least two biological replicates were analysed, and all samples were run in at least two technical replicates. Primers are listed in supporting information table **S1**. Samples were run using two reference genes, ACTIN and PP2A3, validation of reference genes were performed using geNorm method (https://genorm.cmgg.be) for DEX addition (supporting information Table S2), and then samples were normalised using PP2A3 reference gene expression based on these results. Relative expression was determined compared with wild-type using the $2^{(-\Delta Ct)}$ analysis method. In situ hybridisations were conducted in wild-type buds according to Zhu et al. (2011).

ChIP-qPCR analysis

Chromatin immunoprecipitation (ChIP) analysis of AMS-DNA complexes in wild-type was as described by Xu et al. (2010), using their polyclonal AMS-specific antibody (generated using a 522bp *AMS* fragment). 1.5g of formaldehyde cross-linked Col-0 buds (0.6 to 1.1mm) were used with the AMS-antibody and no antibody control. A small aliquot of sonicated DNA prior to immunoprecipitation was used as an input control. qRT-PCR was performed with 'Input control' and 'no antibody control' samples included in the analysis. All samples were run with at least two biological replicates and at least two technical replicates. Quantification involved normalisation of the cycle threshold (Ct) for each sample by subtracting the Ct of the input control; fold enrichment was calculated by subtracting the Ct value of the control (no-antibody).

Electrophoretic mobility shift assay (EMSA)

The recombinant GST-AMS protein was prepared using pGEX-4T-1 plasmid (GST-AMS-F/R – supplemental table S1). DIG-EMSA probes were synthesised by PCR using E-box promoter segments and labelled with digoxigenin (DIG) Dig-dUTP (Roche Diagnostics). DNA binding reactions were performed according to Wang et al. (2002) with minor modifications. Detection of the electrophoretic bands was performed by alkaline phosphatase conjugated anti-DIG antibody.

Tapetum cell sorting

Inflorescences from the tapetum specific A9prom:GFP line (Paul et al. 1992) (kindly donated by Prof. Roderick Scott) and wild-type (Col-0) were collected and pooled from 20 plants (with at least 4 biological replicates), and plant cell walls were digested (Protoplast solution: 600mM mannitol, 2mM $MgCl_2$, 0.1% BSA, 2mM $CaCl_2.2H_2O$, 2mM MES hydrate, 10mM KCl and pH 5.5; with enzymes 1% Cellulase R-10, 0.1% Pectolyase, 1% Hemicellulase, 1.5% Pectinase) at 35^{o}C, shaking at 85 rpm for 1 hour to release protoplasts. Remnants of the buds were removed by filtering through a 70µm sieve. The solution was then centrifuged (6 min, 200g) and the pellet resuspended in fresh protoplast solution. This was then filtered through 70µm and then 40µm sieves, before flow cytometry (FACS). Samples were sorted using a Beckman Coulter Astrios EQ Flow cytometer, equipped with a 488nm laser and 529/28nm band pass filter for GFP/YFP fluorescence. Cells were gated by forward and side scatter profile, and doublet excluded by forward scatter height vs area analysis. GFP fluorescence was identified as signal above wild-type (GFP negative – Col-0) control and cells sorted into protoplast solution. Cells were double sorted to achieved high purity by first using an enrich mode followed by a purify sort mode, this gave a yield of 1000 cells which was 0.2% of the initial input. FACS-sorted cells then had RNA extracted using Arcturus PicoPure RNA isolation Kit following manufacturer's instructions (ThermoFisher Scientific, UK); cDNA synthesis and qRT-PCR expression analysis was performed as stated earlier.

Accession Numbers

Arabidopsis Genome Initiative locus identifiers for the genes described: *AMS* (At2g16910), *ASY1* (At1g67370), *ZYP1* (At1g22260), *DYT1* (At4g21330), *TDF1* (At3g31050), *MS188/MYB80* (At5g56110), *MS1* (At5g22260) *SPO11* (At1g63990), *ATM* (At3g48190), *ATR* (At5g40820), *SHOC1* (At5g52290), *MS5* (At4g20900), *MPS1/PRD2* (At5g57880), *TPR-like* (At1g04770), *T21.H19* (At5g16280), *ML1* (At5g61960), At1g33420.

RESULTS

ams mutants show defects in tetrad formation

Abnormalities in *ams* are first detectable during meiosis in TEM sections; in pre-meiosis the PMC and tapetal cells appeared similar in both wild-type and *ams* (Fig. **1a-b;** Supporting Information Fig. **S1a-b**). During meiosis in wild-type, the cytoplasm of the tapetum cells became condensed and deeply stained (Fig. **1c**; Supporting Information Fig. **S1c**), whereas in *ams* the tapetum cells were swollen with abnormally large vacuoles (Fig. **1d, f**; Supporting Information Fig. **S1d**) and only a few lipidic tapetosomes and elaioplasts. The connections between the tapetum cells in the *ams* mutant also appeared impaired, flattened (Fig. **1d, f**), and less regular than the connections in the wild-type (Fig. **1c, e**). Abnormal cytokinesis occurred in the *ams* meiocytes (Fig. **1h**), with irregular tetrad formation and abnormal callose wall (Fig. **1f, h, j**; Supporting Information Fig. **S1d,f**), in comparison to the wild-type callose wall and tetrad formation (Fig. 1g).

Progression of the early meiosis stages of chromosome pairing and synapsis is not disrupted in *ams* anthers

To uncover the mechanism leading to abnormal tetrads in *ams* we conducted a detailed investigation of chromosome behaviour during meiosis, in *ams* and in other tapetum mutants that are up- and downstream of *AMS*. Meiotic chromosome spreads were prepared using Pollen Mother Cells (PMC) isolated from the *ams*, *dyt1*, *tdf1*, *ms188* and *ms1* mutants and compared to wild-type. In wild-type, chromosome dynamics occurred as expected with metaphase I, metaphase II and telophase II stages having correct chromosome alignment and synapsis, leading to normal tetrad formation (Fig. **2**). These early meiosis stages appeared to occur normally in the mutants, however in *ams*, *tdf1* and *dyt1* abnormal tetrad positioning of nuclei/unbalanced tetrads were frequently seen (26% *ams*, *33% tdf1* and 60% *dyt1*), whilst the downstream mutants (*ms188* and *ms1*) exhibited normal nuclei positioning within the tetrads (Fig. **2; Supporting Information Fig. S2**). This suggests that while early meiotic progression occurs normally there are some defects in the final progression to tetrad formation in *ams*, *tdf1*, and *dyt1*.

We further confirmed that early meiotic events were progressing normally by immunolocalisation using key meiotic proteins, ASY1 (ASYNAPTIC 1) and ZYP1, which are required for normal meiotic progression and crossover formation (Armstrong et al. 2002; Higgins et al. 2005). No differences

were observed in the localisation of ASY1 and ZYP1 proteins between wild-type and *ams* PMCs (Fig. **3a**). Nuclear envelope (NE) formation can impact on meiotic progression as shown in the *sun1* and *sun2* double mutants which have meiotic defects and exhibit a delay in progression of meiosis and an absence of full synapsis (Varas et al. 2015), we therefore analysed immunolocalisation of AtSUN2 (SAD2/UNC-48 DOMAIN PROTEIN 2) to determine if NE formation was altered in *ams* . The integrity of the NE structure appeared similar and regular in both the wild-type and *ams* mutant suggesting the nuclear envelope forms normally in *ams* (Fig. **3b**).

Defects in radial microtubule arrays (RMAs) were observed in the *ams* mutant

To understand the timing of meiotic aberrations in *ams* we looked at spindle assembly using immunolocalisation of alpha-tubulin during both early and late stages of meiosis. During early stages around Prophase I, wild-type and *ams* meiocytes had very similar perinuclear microtubules arrangements (Fig. **4a,b**), no abnormalities were also observed later during metaphase I with *ams* also showing normal spindle morphology (Fig. **4c,d**). These data suggest that early meiosis is not affected in the *ams* mutant. However, normal single microspores are not formed in *ams*, and it is evident that the tetrad stage is unstable with defects observed during cytokinesis (Fig **1f**). Meiosis cytokinesis depends on the formation of radial microtubule arrays (RMAs) through interaction of actin filaments and microtubules with the microtubule organising centres on the surface of telophase II nuclei De Storme and Geelen (2013). During the late tetrad stage, defects in RMAs were analysed using an alpha-tubulin marker, with disorganisation of RMA observed in *ams* (Fig. **4f**). This disorganisation was also seen in the *AMS* upstream mutants, *dyt1* and *tdf1* (Fig. **4g,h**), but not in the down-stream *ms188* mutant (Fig. **4i**). Disorganisation of RMAs is linked to abnormal nuclei positioning within the tetrad, resulting in the formation of unbalanced tetrads, such as the 'triad' distribution of the four nuclei (meiotic restitution), due to disorganisation of microtubules forming between the nuclei. This phenotype was observed in the *ams*, *dyt1* and *tdf1* mutants which all fail to express *AMS*, but not in the later mutant *ms188* (Fig. **4**), this suggests that functional *AMS* may play a key role in the control of cytokinesis and RMA organisation which allows normal tetrad formation.

Callose cell wall is abnormal in *ams* mutant tetrads

Disorganisation of the RMA can affect the microspore cell wall as it mediates cell plate formation, therefore aniline blue staining and analysis of the developing callose cell wall surrounding the tetrads was conducted. Callose wall production was initiated normally in *ams* (Fig. **5a-b**), however callose staining was weaker than observed in wild-type (Fig. **5b**). *GLUCAN SYNTHASE LIKE 1 (GSL1)*, an essential callose synthase in pollen development (Enns et al. 2005), showed slightly reduced expression at the meiotic stage in the *ams* mutant (FlowerNet: www.cpib.ac.uk/anther (Pearce et al.

2015)), which may be associated with the reduced callose staining. There were also defects observed in subsequent callose deposition and cell wall organisation in *ams* (Fig. **1h and 5d**). This disorganisation of the callose cell wall was also observed in the upstream male sterile mutants, *dyt1* and *tdf1* (Fig. **5e,f**), but not in downstream *ms188* and *ms1* mutants (Fig. **5g,h**). This may be a direct consequence of the disorganisation of the RMA, or that AMS itself plays an important role in callose cell wall deposition as previously proposed (Xu et al. 2010; Xu et al. 2014). Alternatively, this could also be a consequence of the tapetum hypertrophy which is observed in *ams* and the upstream mutants *tdf1* and *dyt1*. As well as disorganisation of callose cell wall in these three mutants, there is also an associated compaction, in the wild-type tetrads are well-separated whereas they are observed adjacent to each other in *ams*, *dyt1* and *tdf1* mutants (Supporting Information Fig. **S3**). This compaction could be due to tapetum hypertrophy, and/or may reflect impaired callose deposition/breakdown, since AMS has been previously reported to directly regulate *A6* (*Anther-specific protein 6*), which has been proposed to act in callose breakdown (Xu et al. 2010; Xu et al. 2014).

Time-course analysis of meiotic progression revealed a significant delay in *ams* mutant

The *ams* mutant exhibits more severe impacts on fertility and a complete male sterile phenotype compared to other RMA and callose mutants, suggesting that AMS has additional impacts on pollen development. The duration of meiosis was therefore observed to see if mistiming of pollen development, with associated abnormal tapetum development, was occurring. A detailed analysis of the temporal progression of meiosis in the *ams* mutant was conducted using 5-ethynyl-2'-deoxyuridine (EdU) labelling of meiocytes, focusing on the timing of meiotic phases compared to wild-type. EdU was successfully incorporated into newly synthesised DNA (pre-meiotic S-phase) in both wild-type and *ams* meiocytes in a 2 hour window of EdU labelling. However, while wild-type progressed through the subsequent stages as expected, the EdU labelled time-course of *ams* meiocytes showed delayed progression after the pachytene stage and retarded entry into the later meiotic stages. Wild-type meiocytes progressed quickly to metaphase I, and tetrads could be detected by 32h from the point of EdU labelling (Fig. **6a**). The *ams* mutant however had prolonged progression through pachytene/diplotene/metaphase I; normal tetrads were only occasionally observed in the mutant however this was not until after 42h (Fig. **6b**) rather than the normal 32h seen in wild-type. This suggests that while early meiosis occurs normally the progression itself is delayed through the stages in *ams*, which may contribute to failure of microspore development by misaligning tapetum and microspore development. This proposed delay in meiotic progression was also indicated by observations of bud sizes; larger buds were seen in *ams* from PMC onwards compared to wild-type, with meiosis occurring in smaller buds in wild-type than in the corresponding stage in *ams* (Supporting Information Fig. **S4**). Increased bud size has been previously linked to prolonged meiosis

in meiotic mutants (Chen et al. 2011b), this further supports the hypothesis of delayed meiotic progression in *ams*.

AMS binds the promoter regions of 6 genes associated with meiosis

Meiotic-associated genes *SPO11* (At1g63990), *ATM* (At3g48190), *ATR* (At5g40820), *SHOC1* (At5g52290), *MS5* (At4g20900), *MPS1/PRD2* (At5g57880), *TPR-like* (At1g04770), *T21.H19* (At5g16280), *ML1* (At5g61960), and At1g33420 (Table 1), showed altered expression in *ams* (Xu et al. 2010) and interaction with AMS protein in preliminary ChIP-Seq studies (data not shown), this suggests that AMS may be involved in direct regulation of these genes. The 1-2kb promoter/upstream sequences of these putative meiosis-associated target genes were examined for motifs by TRANSFAC (Transcription Factor Binding Sites) tool (www.biobase-international.com) for presence of AMS binding E-box elements. At least three E-box binding motifs were observed for each target (Fig. **7a**), no other enrichments of common motifs were identified. These regions were used to generate 150-250bp PCR fragments to test for AMS binding to the target promotor regions by ChIP-PCR analysis.

Three independent ChIP experiments were conducted to test for enrichment of the target fragments in DNA immunoprecipitated using an AMS antibody (previously generated for ChIP by Xu *et al*., 2010). The enrichment was calibrated to a positive control of *WBC27* (Xu *et al*., 2010). All 10 genes tested showed enrichment by ChIP-PCR analysis and therefore may be direct AMS targets, however six of these genes *(ATR, MPS1/PRD2, TPR-like, T21.H19, ML1, At1g33420*) showed significant enrichment equivalent or greater than that observed for the positive control *WBC27* (Fig. **7b**). Electrophoretic Mobility Shift Assay (EMSA) was subsequently employed to confirm AMS binding to the promoters of 4 of these putative targets. Purified AMS protein was used to probe E-box rich promoter fragments of the target genes. Retardation was seen with all the genes tested (Fig. **7c**), indicating positive protein-DNA interactions. To demonstrate binding specificity, a 10- fold and 100-fold excess of unlabelled probe was added to the EMSA reaction as competitor. The specific complex was greatly reduced by the addition of the unlabelled competitors, particularly for *ATR, TPR-like* and *ML1*, thus confirming the specificity of interactions between AMS protein and the E-box enriched promoter fragments.

AMS acts as a regulator of meiosis putative AMS targets

Five of the meiosis-associated putative AMS target genes were further analysed for their expression profiles by qRT-PCR in unopened buds. All of these genes showed up-regulated expression in the *ams* mutant compared to wild-type, which was normalised to 1 to aid comparison (Fig. **7d**) suggesting that AMS may negatively regulate the expression of these putative targets. The effect of functional AMS induction was then tested using a dexamethasone (DEX) inducible AMS construct (AMSprom:AMS-GR-YFP from Ferguson *et al.*, 2017), which 24hr after DEX treatment resulted in AMS protein localised to the nucleus and a reduction in the expression of all the putative targets when compared to AMS-GR-YFP prior to DEX treatment (normalised to 1 to aid comparison), with TPR-like showing the strongest association (Fig. **7d**).

AMS has been detected in the tapetum with no meiocyte expression observed (Ferguson et al. 2017), therefore expression analysis was performed on the meiotic-associated genes to determine if these target genes were also present in the tapetum. Isolated tapetum cells, expressing the tapetum-specific A9prom:GFP transgene ((Paul et al. 1992) kindly provided by Prof Roderick Scott), were enzymatically separated and fluorescence-activated cell sorted (FACS) based on the GFP marker, and then used for qRT-PCR. Enrichment of the selected meiotic-associated AMS target genes was seen within the tapetum enriched samples (Supporting Information Fig. **S5a**). In these tapetum cells all of the meiotic genes tested, except for MPS1, were present, however early meiotic genes such as *ML1*, *TPR-like* and *At1g33420* showed higher enrichment. This may be a reflection of the fact the early meiotic cells were easier to release during enzyme digestion for cell sorting, since this was also seen in the strong enrichment of *DYT1* (early meiosis), compared to *AMS* (late meiosis). Tapetum-localisation was further confirmed for one of these genes, *ML1*, through *in* situ hybridisation (Supporting Information Fig **S5b-d**). This co-localisation of expression further supports the potential direct interaction between AMS and *ATR, TPR-like, T21.H19, ML1, At1g33420* within the tapetum. This suggests that AMS repression of these targets may be needed for progression of the final stages of meiosis, but that this interaction may occur within the tapetum, but the subsequent impact of this is manifested in the gametophyte.

DISCUSSION

AMS is a bHLH transcription factor that acts as a key player in tapetum development via the direct regulation of many genes (Ferguson et al., 2017) and thus plays an important role in viable pollen formation, with major impacts on late meiotic events as well as its well-characterised later role during pollen wall formation.

Callose wall formation is impaired in *ams* during meiosis

In the *ams* mutant early meiosis initiates normally, however there is a failure during late meiosis with abnormalities such as callose wall formation observed, which ultimately leads to microspore degeneration. Callose wall deposition is important for establishing the matrix for pollen wall formation and the generation of viable pollen. This change in callose wall formation may be a direct effect of the lack of *ams* as AMS itself plays an important role in callose cell wall deposition as previously proposed (Xu et al. 2010; Xu et al. 2014). Alternatively, tapetum hypertrophy occurs in the *dyt1, tdf1* and *ams* mutants and appears to result in it filling the locule and squeezing the meiocytes, this could potentially impact the callose wall formation/dissolution, especially as the meiocytes appear close together in these three mutants, rather than well separated as in wild-type (Supporting Information Fig. S3). Mutants in callose deposition at the developing cell plate such *gsl1/gsl5* double mutants, have no callose wall in-between the developing tetrads resulting in problems in tetrad dissociation, failed cytokinesis and pollen abortion, nevertheless they are able to produce some abnormal larger pollen with multiple nuclei (Enns et al. 2005). However, the phenotype observed in *ams* is more severe, with no single microspores formed and full sterility, suggesting that AMS is playing an additional role(s) in late meiosis development, leading to failure of cytokinesis and single microspore formation. This is also evident from previous rescue experiments using a DEX-inducible AMS construct, which required multiple DEX treatments to ensure that functional AMS was present at multiple stages to facilitate viable pollen formation (Ferguson et al., 2017). Along with callose, exine deposition is also critical for ultimate pollen viability, with callose and exine mutant phenotypes leading to pollen degeneration (Xu et al. 2014). AMS has a well-established role in exine formation, which may explain why there is ultimately pollen degeneration in this mutant. However here we have shown it also has an earlier role, which is associated with late meiotic progression, causing abnormalities in intersporal callose deposition, during cytokinesis, RMA formation and cytokinesis.

AMS plays a role in late meiotic progression through RMA formation and cytokinesis

We have found that early meiosis initiates normally in *ams*, but exhibits delayed progression from the pachytene stage, and then there is a failure during late meiosis with defects in RMA, cytokinesis and intersporal callose wall formation. Mutants such as *tes/stud/Atnack2, mpk4* and *aesp* have problems with disorganised RMA and therefore loss of callose deposition, nevertheless they can still form monad pollen with multiple nuclei despite disorganised RMA and loss of intersporal callose deposition (Yang et al. 2003; Zeng et al. 2011). The *ams* mutant however has a more severe phenotype with meiocytes that are unable to progress past cytokinesis, compared to other mutants

involved in RMA formation. Cold stress has also been shown to impact on RMA organisation, resulting in diploid and polyploid pollen De Storme et al. (2012), and Spielman et al. (1997) have showed that a kinesin mutant with failed cytokinesis led to monad formation, forming tetraploid, or multi-sperm pollen. Defects in RMA do not typically result in inviable pollen, therefore the observed microspore degeneration in *ams* is unlikely to be the result of the callose/RMA/cytokinesis defect alone. The RMA/triad phenotype of *ams* is similar to a hypomorphic *MPS1/PRD2* mutant (Walker et al. 2018), and therefore affecting the expression of these genes may explain part of the *ams* meiotic phenotype.

AMS directly represses meiosis-associated genes to mediate crosstalk between the tapetum and meiocytes

We have shown that selected meiosis-associated genes are directly repressed by AMS and suggest that this may be essential for late-stage meiosis progression (Fig. **8**). AMS is a tapetal expressed protein (Ferguson et al., 2017), whereas meiosis is occurring within the developing meiocytes, however, we have shown by qRT-PCR of FACS-sorted tapetum cells and *in situ* hybridisation, that these meiotic-associated genes are also expressed in the tapetum. Recent work (Li et al. 2017) using laser microdissection also shows expression of *ML1*, *MPS1/PRD2* and *At1g33420* in stage 6-7 tapetum cells. *ML1* has also previously been shown to be expressed in tapetum cells and meiocytes (Kaur et al. 2006). AMS and the target genes are therefore all expressed within the tapetum and thus AMS may be directly interacting with the promoters of these genes in the tapetum to change their expression to enable meiotic progression and meiocyte development. AMS is known to be a positive regulator of expression, therefore repression by AMS may be caused by the binding of AMS to the E-boxes on the target promoters and blocking access to other transcriptional regulators, and thus causing their down-regulation. We show a clear reduction of these meiosis-associated gene transcripts as a consequence of AMS expression, which suggests that their tapetum expression needs to be halted for meiosis to progress and that AMS is coordinating this regulation. This may be due to the movement of RNAs or proteins from the tapetum to the Pollen Mother Cells, since it is indicated that such actions occur as part of the crosstalk between the tapetum and meiocytes (Lei and Liu 2019), although the factors involved in this are unknown. The cellulose in the tapetum walls is lost prior to meiosis (Matsuo et al. 2013), thus potentially favouring the movement of materials between the tapetum, anther locule and meiocytes at this stage.

Recently it has been shown that gene targeting siRNAs are produced in tapetal cells and transported into meiocytes possibly through plasmodesmata that connect these cells during early meiosis (Long et

al. 2021). Therefore, an alternative hypothesis is that AMS may play a role in activating RNA-mediated gene regulation, such as large intergenic non-coding RNAs (lincRNAs). Recent work (Ono et al. 2018) has indicated that EAT1, a rice tapetal bHLH transcription factor, is able to activate lincRNAs, which are possible mobile signals between the tapetum and reproductive cells and may facilitate negative gene regulation. EAT1 has been shown to have a bimodal expression similar to AMS and also to cause delayed and asynchronous male meiosis in regard to spike size (Ono et al. 2018). We observed this delay and asynchronous meiosis in the *ams* mutant, with increased bud sizes seen in *ams* compared to the corresponding meiosis stages in wild-type buds (Supporting Information Fig. **S4**). The negative regulation of meiotic genes to allow tight control of meiosis and tapetal development may be a way to synchronise the development of these two cell types.

Correct and timely tapetal development has been shown to be very important for the establishment of microspores, and early tapetum mutants such as *dyt1* and *tdf1* mutants also present similar phenotypes to *ams* with RMA disorganisation, failed cytokinesis and abnormal callose wall formation, suggesting that loss of AMS in the upstream transcription factor mutants *dyt1* and *tdf1* may be the principal cause for these phenotypes (Fig. **8**). This is supported by the phenotypes of the male sterile mutants downstream of *ams* that do not exhibit these defects, with normal RMA organisation and callose deposition seen in *ms188* and *ms1* mutants. All three of these early mutants (*dyt1*, *tdf1* and *ams*) lack a normal tapetum during this key stage (Zhang *et al.*, 2006; Zhu *et al.*, 2008), indicating that a functional tapetum is critical for completion of meiosis. This suggests that tapetum signals regulating the final progression of meiosis are absent in *ams*, and therefore the *dyt* and *tdf1* mutants. TEM sections of *ams* tapetum cells indicate that they are highly vacuolated and expanded; this occurs significantly earlier than wild-type, with vacuolation from meiosis onwards and a lack of functional tapetum cells, which are important for providing callose synthase, callase, cellulose and possibly energy in the form of sugars for microspore development (Fig. **1c-j**). We have observed that the *ams* mutant tapetum has very low amounts of lipidic tapetosomes and elaioplasts, which may impair its ability to provide the necessary building blocks for the early cellulose wall production. The tapetum is grossly enlarged (hypertrophy) at this stage in the *dyt1*, *tdf1* and *ams* mutants, appearing to fill the locule and squeeze the meiocytes, which may also impact on normal RMA formation, callose deposition and cytokinesis within the developing meiocytes. Tapetum development does not appear synchronised with the adjacent tetrad formation in *ams* compared to wild-type, suggesting that tapetum development is important for fulfilling the requirements of the meiocytes, which may therefore explain why *ams* exhibits delayed meiotic progression and incomplete pollen wall production. In the future it would be interesting to try to distinguish between the impact of the loss of *ams* and tapetum hypertrophy with its effect on callose formation, RMAs, cytokinesis, tetrad

formation and meiotic progression, for example by testing the impact of DEX-induced AMS expression during early microspore development/meiosis in the *ams, dyt1* and *tdf* mutants. As well as looking at hypertrophic tapetum mutants that are not directly linked to reduction in *ams* expression.

CONCLUSIONS

In summary, we have shown that meiosis initiates and progresses normally in the *ams* mutant until the pachytene stage, where the progression is delayed, with problems apparent at late meiosis stages, with delayed completion of meiosis, disorganised RMA, defective cytokinesis, followed by tetrad collapse and degeneration observed. This, and the subsequent failure in callose and exine development may be the principal causes of the failure of pollen development in *ams*. We have shown that selected meiosis-associated genes are directly repressed by AMS and that this is likely to occur in the tapetum, but that this down-regulation impacts on the meiocytes and is essential for late-stage meiotic progression (Fig. **8**). AMS is critical for cytokinesis and RMA organisation to allow correct tetrad formation, alongside its established role later in pollen wall development. The work presented here explains the function of our previously reported early peak of AMS protein (Ferguson et al. 2017), and identifies a new role for AMS during late meiosis. This indicates that AMS has a dual function, with a previously unreported role during early pollen development in controlling late meiotic progression, as well as its subsequent role as a master regulator of pollen wall biosynthesis and formation. Despite gametophytic control of initiation of Pollen Mother Cell meiosis, there is clear maternal regulation via the tapetum. This work identifies AMS as a key player in the crosstalk between the gametophyte and sporophytic tissues, which is essential to enable synchronous development of tapetum and microspores for functional pollen formation.

ACKNOWLEDGEMENTS

The *dyt1*, *tdf1*, *myb80* (*ms188*) mutant lines were kindly shared by Dr. ZhongNan Yang.

AUTHOR CONTRIBUTIONS

Z.A.W designed the research; I.F., A.C.T., G.V.B., B.L., X.J., WY performed the research; J.D.H. assisted I.F. and A.C.T.; I.F., A.C.T., J.D.H., B.L., D.G., Z.A.W. analysed the data; Z.A.W., I.F., A.C.T. wrote the manuscript; Z.A.W., A.C.T., G.V.B., J.D.H., D.Z., B.L., D.G. reviewed and edited the manuscript. Z.A.W. agrees to serve as the author responsible for contact and ensures communication.

CONFLICT OF INTEREST

The authors have no conflicts to declare.

FUNDING INFORMATION

This research was supported by the Biotechnology and Biological Sciences Research Council (Grant Reference BB/J001295/1); IF was supported by a BBSRC studentship Award Reference 976074; Bing Liu was supported by the China Scholarship Council.

DATA AVAILABILITY

All data supporting the findings of this study are available within the paper and within its supplementary materials published online.

REFERENCES

Armstrong SJ, Caryl AP, Jones GH, Franklin FC (2002) Asy1, a protein required for meiotic chromosome synapsis, localizes to axis-associated chromatin in Arabidopsis and Brassica. Journal Cell Science 115 (Pt 18):3645-3655

Blatch GL, Lassle M (1999) The tetratricopeptide repeat: a structural motif mediating protein-protein interactions. BioEssays : news and reviews in molecular, cellular and developmental biology 21:932-939

Caryl AP, Jones GH, Franklin FCH (2003) Dissecting plant meiosis using *Arabidopsis thaliana* mutants. Journal of Experimental Botany 54 (380):25-38

Chang F, Wang Y, Wang S, Ma H (2011) Molecular control of microsporogenesis in Arabidopsis. Current Opinion Plant Biology 14 (1):66-73. doi:10.1016/j.pbi.2010.11.001

Chen W, Yu XH, Zhang K, Shi J, Schreiber L, Shanklin J, Zhang D (2011a) Male Sterile 2 Encodes a Plastid-localized Fatty Acyl ACP Reductase Required for Pollen Exine Development in Arabidopsis thaliana. Plant Physiology 157 (2):842-853. doi:10.1104/pp.111.181693

Chen Z, Higgins JD, Hui JT, Li J, Franklin FC, Berger F (2011b) Retinoblastoma protein is essential for early meiotic events in Arabidopsis. EMBO Journal 30 (4):744-755. doi:10.1038/emboj.2010.344

Cui J, You C, Zhu E, Huang Q, Ma H, Chang F (2016) Feedback Regulation of DYT1 by Interactions with Downstream bHLH Factors Promotes DYT1 Nuclear Localization and Anther Development. Plant Cell 28 (5):1078-1093. doi:10.1105/tpc.15.00986

Culligan K, Tissier A, Britt A (2004) ATR Regulates a G2-Phase Cell-Cycle Checkpoint in *Arabidopsis thaliana*. The Plant Cell 16:1091-1104

de Muyt A, Pereira L, Vezon D, Chelysheva L, Gendrot G, Chambon A, Lainé-Choinard S, Pelletier G, Mercier R, Nogué F, Grelon M (2009) A high throughput genetic screen identifies new early meiotic recombination functions in Arabidopsis thaliana. PLoS Genetics 5 (9)::e1000654. doi:10.1371/journal.pgen.1000654.

De Storme N, Copenhaver GP, Geelen D (2012) Production of diploid male gametes in Arabidopsis by cold-induced destabilization of postmeiotic radial microtubule arrays. Plant Physiology 160 (4):1808-1826. doi:10.1104/pp.112.208611

De Storme N, Geelen D (2013) Cytokinesis in plant male meiosis. Plant Signaling & Behavior 8 (3):e23394. doi:10.4161/psb.23394

Enns LC, Kanaoka MM, Torii KU, Comai L, Okada K, Cleland RE (2005) Two callose synthases, GSL1 and GSL5, play an essential and redundant role in plant and pollen development and in fertility. Plant Molecular Biology 58 (3):333-349. doi:10.1007/s11103-005-4526-7

Ferguson AC, Pearce S, Band LR, Yang C, Ferjentsikova I, King J, Yuan Z, Zhang D, Wilson ZA (2017) Biphasic regulation of the transcription factor ABORTED MICROSPORES (AMS) is essential for tapetum and pollen development in Arabidopsis. New Phytologist 213 (2):778-790. doi:10.1111/nph.14200

Fu Z, Yu J, Cheng X, Zong X, Xu J, Chen M, Li Z, Zhang D, Liang W (2014) The Rice Basic Helix-Loop-Helix Transcription Factor TDR INTERACTING PROTEIN2 Is a Central Switch in Early Anther Development. The Plant Cell 26 (4):1512-1524. doi:10.1105/tpc.114.123745

Garcia V, Bruchet H, Camescasse D, Granier F, Bouchez D, Tissier A (2003) AtATM is essential for meiosis and the somatic response to DNA damage in plants. The Plant Cell 15 (1):119-132

Glover J, Grelon M, Craig S, Chaudhury A, Dennis E (1998) Cloning and characterization of *MS5* from *Arabidopsis*: a gene critical in male meiosis. Plant Journal 15 (3):345-356

Hartung F, Wurz-Wildersinn R, Fuchs J, Schubert I, Suer S, Puchta H (2007) The catalytically active tyrosine residues of both SPO11-1 and SPO11-2 are required for meiotic double-strand break induction in Arabidopsis. The Plant Cell 19 (10):3090-3099. doi:10.1105/tpc.107.054817

Higgins JD, Sanchez-Moran E, Armstrong SJ, Jones GH, Franklin FCH (2005) The Arabidopsis synaptonemal complex protein ZYP1 is required for chromosome synapsis and normal fidelity of crossing over. Genes & Development 19 (20):2488-2500. doi:10.1101/gad.354705

Higgins JD, Wright KM, Bomblies K, Franklin FC (2014) Cytological techniques to analyze meiosis in Arabidopsis arenosa for investigating adaptation to polyploidy. Frontiers Plant Science 4:546. doi:10.3389/fpls.2013.00546

Jiang H, Wang FF, Wu YT, Zhou X, Huang XY, Zhu J, Gao JF, Dong RB, Cao KM, Yang ZN (2009) MULTIPOLAR SPINDLE 1 (MPS1), a novel coiled-coil protein of Arabidopsis thaliana, is required for meiotic spindle organization. Plant Journal 59 (6):1001-1010. doi:10.1111/j.1365-313X.2009.03929.x

Kaur J, Sebastian J, Siddiqi I (2006) The Arabidopsis-mei2-like genes play a role in meiosis and vegetative growth in Arabidopsis. The Plant Cell 18 (3):545-559. doi:10.1105/tpc.105.039156

Lei X, Liu B (2019) Tapetum-Dependent Male Meiosis Progression in Plants: Increasing Evidence Emerges. Frontiers Plant Science 10:1667. doi:10.3389/fpls.2019.01667

Li DD, Xue JS, Zhu J, Yang ZN (2017) Gene Regulatory Network for Tapetum Development in Arabidopsis thaliana. Frontiers Plant Science 8:1559. doi:10.3389/fpls.2017.01559

Liu J, Qu LJ (2008) Meiotic and mitotic cell cycle mutants involved in gametophyte development in Arabidopsis. Molecular Plant 1 (4):564-574. doi:10.1093/mp/ssn033

Liu L, Fan XD (2013) Tapetum: regulation and role in sporopollenin biosynthesis in Arabidopsis. Plant Molecular Biology 83 (3):165-175. doi:Doi 10.1007/S11103-013-0085-5

Long J, Walker J, She W, Aldridge B, Gao H, Deans S, Vickers M, Feng X (2021) Nurse cell--derived small RNAs define paternal epigenetic inheritance in Arabidopsis. Science 373 (6550). doi:10.1126/science.abh0556

Macaisne N, Vignard J, Mercier R (2011) SHOC1 and PTD form an XPF-ERCC1-like complex that is required for formation of class I crossovers. Journal Cell Science 124:2687-2691

Matsuo Y, Arimura S, Tsutsumi N (2013) Distribution of cellulosic wall in the anthers of Arabidopsis during microsporogenesis. Plant Cell Reports 32 (11):1743-1750. doi:10.1007/s00299-013-1487-1

Ono S, Liu H, Tsuda K, Fukai E, Tanaka K, Sasaki T, Nonomura KI (2018) EAT1 transcription factor, a non-cell-autonomous regulator of pollen production, activates meiotic small RNA biogenesis in rice anther tapetum. PLoS Genetics 14 (2):e1007238. doi:10.1371/journal.pgen.1007238

Paul W, Hodge R, Smartt S, Draper J, Scott R (1992) The isolation and characterisation of the tapetum-specific Arabidopsis thaliana A9 gene. Plant Mol Biology 19 (4):611-622. doi:10.1007/BF00026787

Pearce S, Ferguson A, King J, Wilson ZA (2015) FlowerNet: a gene expression correlation network for anther and pollen development. Plant Physiology 167 (4):1717-1730. doi:10.1104/pp.114.253807

Sanders PM, Bui AQ, Weterings K, McIntire KN, Hsu YC, Lee PY, Truong MT, Beals TP, Goldberg RB (1999) Anther developmental defects in Arabidopsis thaliana male-sterile mutants. Sexual Plant Reproduction 11 (6):297-322

Shi J, Cui M, Yang L, Kim YJ, Zhang D (2015) Genetic and Biochemical Mechanisms of Pollen Wall Development. Trends Plant Science 20 (11):741-753. doi:10.1016/j.tplants.2015.07.010

Sorensen AM, Krober S, Unte US, Huijser P, Dekker K, Saedler H (2003) The *Arabidopsis ABORTED MICROSPORES (AMS)* gene encodes a MYC class transcription factor. Plant Journal 33 (2):413-423

Spielman M, Preuss D, Li FL, Browne WE, Scott RJ, Dickinson HG (1997) TETRASPORE is required for male meiotic cytokinesis in Arabidopsis thaliana. Development 124 (13):2645-2657

Stacey NJ, Kuromori T, Azumi Y, Roberts G, Breuer C, Wada T, Maxwell A, Roberts K, Sugimoto-Shirasu K (2006) Arabidopsis SPO11-2 functions with SPO11-1 in meiotic recombination. Plant Journal 48 (2):206-216. doi:10.1111/j.1365-313X.2006.02867.x

Varas J, Graumann K, Osman K, Pradillo M, Evans DE, Santos JL, Armstrong SJ (2015) Absence of SUN1 and SUN2 proteins in Arabidopsis thaliana leads to a delay in meiotic progression and defects in synapsis and recombination. Plant Journal 81 (2):329-346. doi:10.1111/tpj.12730

Walker J, Gao H, Zhang J, Aldridge B, Vickers M, Higgins JD, Feng X (2018) Sexual-lineage-specific DNA methylation regulates meiosis in Arabidopsis. Nature Genet 50 (1):130-137. doi:0.1038/s41588-017-0008-5

Wang HD, Iacoangeli A, Popp S, Muslimov IA, Imataka H, Sonenberg N, Lomakin IB, Tiedge H (2002) Dendritic BC1 RNA: Functional role in regulation of translation initiation. Journal Neuroscience 22 (23):10232-10241

Wang K, Guo ZL, Zhou WT, Zhang C, Zhang ZY, Lou Y, Xiong SX, Yao XZ, Fan JJ, Zhu J, Yang ZN (2018) The Regulation of Sporopollenin Biosynthesis Genes for Rapid Pollen Wall Formation. Plant Physiology 178 (1):283-294. doi:10.1104/pp.18.00219

Xiong SX, Lu JY, Lou Y, Teng XD, Gu JN, Zhang C, Shi QS, Yang ZN, Zhu J (2016) The transcription factors MS188 and AMS form a complex to activate the expression of CYP703A2 for sporopollenin biosynthesis in Arabidopsis thaliana. Plant Journal 88 (6):936-946. doi:10.1111/tpj.13284

Xu J, Ding ZW, Vizcay-Barrena G, Shi JX, Liang WQ, Yuan Z, Werck-Reichhart D, Schreiber L, Wilson ZA, Zhang DB (2014) ABORTED MICROSPORES Acts as a Master Regulator of Pollen Wall Formation in Arabidopsis. The Plant Cell 26 (4):1544-1556. doi:Doi 10.1105/Tpc.114.122986

Xu J, Yang C, Yuan Z, Zhang D, Gondwe MY, Ding Z, Liang W, Zhang D-B, Wilson ZA (2010) The ABORTED MICROSPORES regulatory network is required for postmeiotic male reproductive development in Arabidopsis thaliana. The Plant Cell 22 (1):91-107. doi:tpc.109.071803 [pii]
10.1105/tpc.109.071803

Yang C-Y, Vizcay-Barrena G, Conner K, Wilson ZA (2007) MALE STERILITY1 is required for tapetal development and pollen wall biosynthesis. The Plant Cell 19 (11):3530-3548

Yang CY, Spielman M, Coles JP, Li Y, Ghelani S, Bourdon V, Brown RC, Lemmon BE, Scott RJ, Dickinson HG (2003) TETRASPORE encodes a kinesin required for male meiotic cytokinesis in Arabidopsis. Plant Journal 34 (2):229-240

Zeng Q, Chen J-G, Ellis BE (2011) AtMPK4 is required for male-specific meiotic cytokinesis in Arabidopsis. Plant Journal 67 (5):895-906. doi:10.1111/j.1365-313X.2011.04642.x

Zhang DB, Yang L (2014) Specification of tapetum and microsporocyte cells within the anther. Current Opinion in Plant Biology 17:49-55. doi:10.1016/j.pbi.2013.11.001

Zhang W, Sun YL, Timofejeva L, Chen C, Grossniklaus U, Ma H (2006) Regulation of *Arabidopsis* tapetum development and function by *DYSFUNCTIONAL TAPETUM (DYT1)* encoding a putative bHLH transcription factor. Development 133:3085-3095

Zhang ZB, Zhu J, Gao JF, Wang C, Li H, Li H, Zhang HQ, Zhang S, Wang DM, Wang QX, Huang H, Xia HJ, Yang ZN (2007) Transcription factor AtMYB103 is required for anther development by regulating tapetum development, callose dissolution and exine formation in Arabidopsis. Plant Journal 52 (3):528-538

Zhao DZ, Wang GF, Speal B, Ma H (2002) The excess microsporocytes1 gene encodes a putative leucine-rich repeat receptor protein kinase that controls somatic and reproductive cell fates in the Arabidopsis anther. Genes Development 16 (15):2021-2031

Zhu J, Chen H, Li H, Gao JF, Jiang H, Wang C, Guan YF, Yang ZN (2008) Defective in Tapetal development and function 1 is essential for anther development and tapetal function for microspore maturation in Arabidopsis. Plant Journal 55 (2):266-277

Zhu J, Lou Y, Xu X, Yang Z-N (2011) A Genetic Pathway for Tapetum Development and Function in Arabidopsis. Journal of Integrative Plant Biology 53 (11):892-900. doi:10.1111/j.1744-7909.2011.01078.x

Table 1: Putative AMS target genes associated with Pollen Mother Cell meiosis

AMS putative target genes	**Gene Name**	**Known function in Arabidopsis**	**Associated References**
At1g63990	*SPO11-2*	Endonuclease responsible for the induction of DNA Double Strand Breaks (DSBs) during meiosis	(Hartung et al. 2007; Stacey et al. 2006)
At5g52290	*SHOC1*	Required for class I cross-overs during meiosis	(Macaisne et al. 2011)
At5g57880	*MPS1/PRD2*	Involved in DNA double strand break formation and spindle organisation in meiocytes, transcript expression reached its highest level in male meiocytes	(Jiang et al. 2009; de Muyt et al. 2009)
At4g20900	*MS5*	Abnormalities after meiosis II in *ms5*, possibly due to disturbances in meiosis I or in proteins of the SC.	(Glover et al. 1998)
At5g61960	*ML1*	Meiotic abnormalities: pairing defects, fragmentation and clumping of chromosomes	(Kaur et al. 2006)
At1g33420	-	RING/FYVE/PHD zinc finger superfamily protein; likely involved in transcription	-
At1g04770	*TPR-like SID2*	48% identity with MS5 family protein	(Blatch and Lassle 1999)
At3g48190	*ATM*	Signal transducer in DNA damage repair machinery, signals the existence of DNA double-strand breaks	(Garcia et al. 2003)
At5g40820	*ATR*	Signals the presence of DNA single-stranded breaks, mostly at stalled replication forks	(Culligan et al. 2004)
At5g16280	*T21.H19*	Tetratricopeptide repeat (TPR)-like superfamily protein; 96.5% identity with *A. lyrata* involved in protein trafficking	-

FIGURE LEGENDS

FIGURE 1. *ams* is male sterile, with abnormal tapetum and tetrads.

TEM anther sections of wild-type (wt) Col-0 (**a, c, e, g, i**) and *ams* mutant (**b, d, f, h, j**). (**a, b**) TEM sections of pollen mother cells (PMC) pre-meiosis and tapetum in wt (**a**) and *ams* (**b**), showing normal tapetum (T) and PMC, middle layer (ML), Endodermis (En), Epidermis (Ep). Meiosis progresses normally in wt (**c, e**), whereas irregularities occur in the *ams* tapetum with pre-vacuolation (v) mutant tapetal cells (**d, f**). Connections between tapetum cells and PMC are seen in wt (**c, e**, arrows), whilst abnormal/compressed connections are seen in the *ams* mutant (**d, f**, arrows). Wild-type (**g**) showing callose cell wall deposition on developing meiocytes with cytokinesis occurring to form tetrads, while *ams* (**h**) has abnormal callose accumulation and separation. Normal tetrads are seen in wt (**i**) stage (Vacuoles: v), whereas abnormal tetrads and highly vacuolated (v) tapetum cells are observed in *ams* (**j**). Scale bar **c, d, g, h** = 5 μm, rest = 10 μm.

FIGURE 2. Male sterile mutants have normal early meiosis development.

4',6-Diamidino-2-phenylindole (DAPI) staining of wild-type (wt) and male sterile mutants *ams*, *dyt1*, *tdf1*, *ms188* and *ms1* meiocytes during male meiosis. The presence of five bivalents is clear at metaphase I and metaphase II in all lines, with correct separation occurring in metaphase II. During telophase II there is the balanced formation of four sets of five chromosomes with the correct formation of tetrads in all lines observed. Scale bar = 10μm.

FIGURE 3. Chromosome pairing, synapsis and nuclear envelope formation appear normal in *ams*.

(a) Localisation of the synaptonemal complex protein ZYP1 (red) and the axis-associated protein ASY1 (green) at zygotene stage in wt and *ams*. The distribution of both proteins appears normal indicating that chromosome pairing and synapsis occur in the absence of AMS. Chromosomes are counterstained with DAPI (blue). Scale bar = 5 μm.

(b) Nucleoporin localisation in wt and *ams* pollen mother cells, similar nuclear envelope expression patterns of AtSUN2 in wild-type and *ams* at telophase II with AtSUN2 (green) antibody, counterstained using DAPI (blue), strongest SUN2 signal was observed in *ams*. Scale bars = 5μm.

FIGURE 4. Spindle formation morphology in wild-type and male sterile meiocytes.

The spindle was detected by immunostaining with anti-α-tubulin antibody (green) and chromosomes were counterstained with DAPI (blue). Tubulin localisation is similar in wt Col-0 and *ams* at prophase I **(a, b)**, with normal spindle morphology during metaphase I in Col-0 **(c)** and *ams* **(d)**. Radial microtubule arrays (RMA) however are disorganised in *ams* **(f)** compared to wt **(e)**, this is also observed in the upstream male sterile mutants *dyt1* **(g)**, *tdf1* **(h)**, but not the downstream mutant *ms188* **(i)**. Nuclei positioning within the tetrad is also unbalanced forming a 'triad' like shape in *dyt1*, *tdf1*, and *ams* **(g-i)**. Scale bar = 5μm.

FIGURE 5. Callose staining of male meiocytes of tapetum defective mutants.

Callose staining of wild-type Col-0 (**a**) and *ams* (**b**) tetrads during meiosis initially showed similar callose production, suggesting normal initiation of callose biosynthesis. Callose deposition, forming thick walls surrounding the tetrads, was subsequently seen in wt **(c)**, whereas this was abnormal and disorganised in *ams* tetrads (**d**), *dyt1* (**e**) and *tdf1* mutants (**f**), whereas the later stage tapetum mutants, *ms188* (**g**) and *ms1* (**h**), showed normal callose deposition and thick, ordered callose layers surrounding the tetrads. Scale bars = 10 μm.

FIGURE 6. Meiotic progression over time in *ams* compared to wild-type.

Detection of EdU labelling in pollen mother cells across a time course of sampled cells (2h, 8h, 18h, 28h, 32h and 42h). EdU Alexa Fluor® 488 (white). (**a**) Wild-type Col-0 showing normal meiotic progression, with tetrads observed after 32h, whilst (**b**) *ams* showed delayed progression through meiosis after pachytene stage, with occasional tetrads observed only after 42h. Scale bar = 10μm.

FIGURE 7. AMS binds directly to the promoters of selected meiotic-associated genes to regulate their expression.

(a) ChIP-qPCR analysis of the enrichment of AMS regulatory targets compared to WBC27 positive control. Predicted E-boxes in the promoter region represented by dark vertical lines and promoter regions analysed by ChIP-qPCR and EMSA represented by dotted line and arrows. **(b)** Fold enrichment represents the fold change in +Ab (antibody) compared with -Ab samples, normalised to WBC27 fold change. qPCR data were gathered from three biological and two technical replicates. Significant changes based on student t-test $P<0.05$ are represented by *. Error bar represent SD. **(c)** EMSA using digoxigenin

(DIG) labelled probes without AMS protein or unlabelled probes (lane 1), lanes 2-4 show AMS protein and DIG labelled probe with increasing amount of competitor DNA (10x, 100x respectively). Gel retardation indicates the binding of the AMS to promoters of the target genes. **(d)** Relative expression values based on qRT-PCR analysis measured in whole inflorescence in wild-type (Col-0), *ams* and AMSprom:AMS-GR-YFP in wt Col-0 background. Showing up-regulation in *ams* mutant and down-regulated in the AMSprom:AMS-GR-YFP line 24 hours after AMS induction by DEX. Expression was normalised to wild-type for *ams* and AMS-GR-YFP without DEX for AMS-GR-YFP 24hr after DEX. Significant changes based on student t-test $P<0.05$ are represented by *. Error bars represent SE.

FIGURE 8. Proposed regulatory network for AMS.

Tapetum regulatory pathway based on network published in Ferguson et al., (2017), AMS is directly regulated by DYT1 through TDF1, and itself directly regulates MS188, which regulates MS1. AMS has a published role in sporopollenin wall formation alongside MS188. We propose that it is the loss of AMS in the early tapetum mutants that cause the phenotypes observed in *ams, tdf1* and *dyt1* mutants, as *ms188* and *ms1* develop normally. We have shown a novel role for AMS in the correct regulation of RMA localisation (green lines in meiocytes) during telophase II, for correct cytokinesis, callose wall deposition (yellow material in meiocyte) to produce a functional tetrad. AMS is also important for fully functional tapetum cells which have a high energy requirement during meiosis (darker background colour representing this, and black dots indicate lipidic tapetosomes and elaioplasts) to provide for the developing pollen. We have shown that AMS appears to directly negatively regulate at least 4 meiosis-associated genes, possibly through interaction in the tapetum, and propose that AMS has a role in the final stages of meiosis through their regulation. v: vacuole; n: nucleus. Arrows: regulation; lines ending with a line: repression; lines with a line ending with circle: protein interactions. Dashed lines indicate a minor role in regulation of network (as predicted by modelling (Ferguson et al. 2017)). Red lines indicate a major role in regulation.

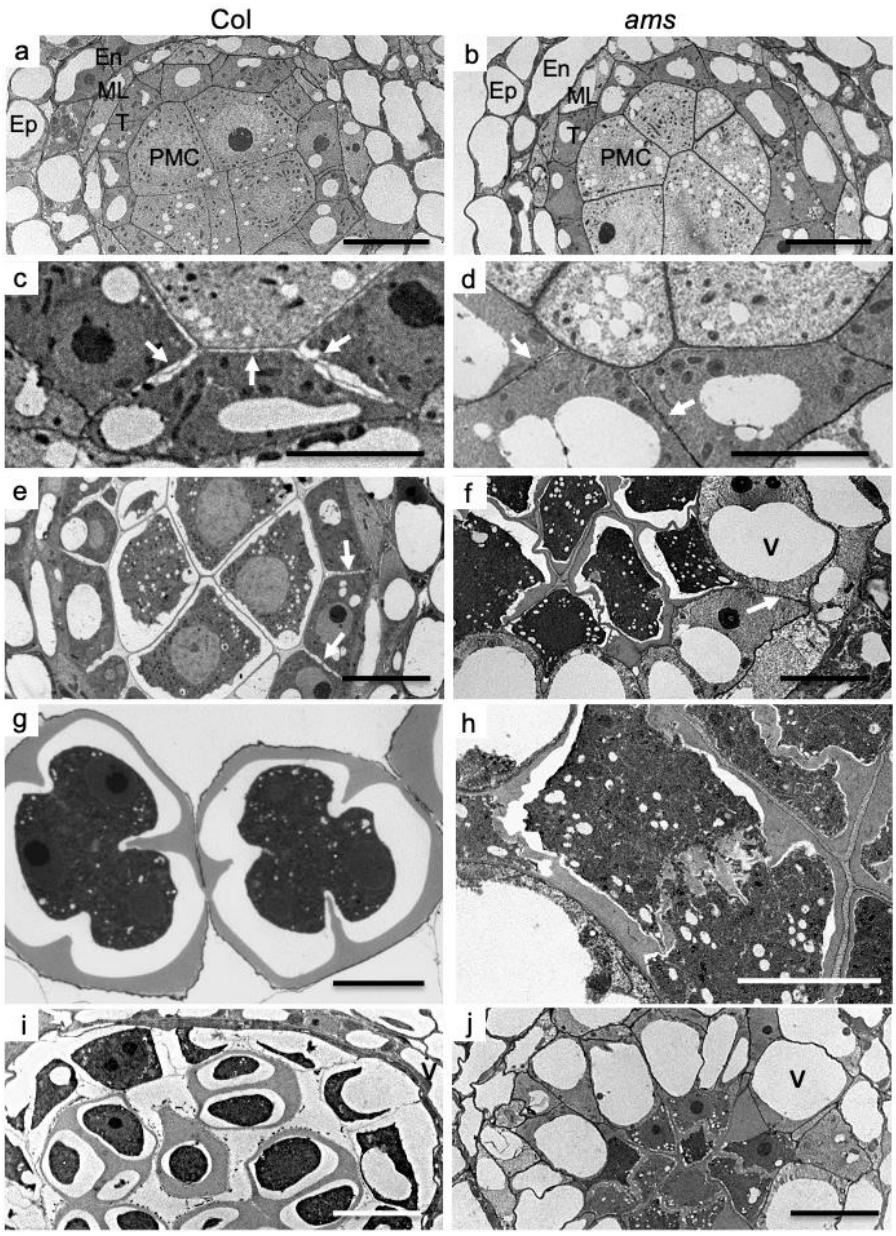

FIGURE 1. *ams* is male sterile, with abnormal tapetum and tetrads.
TEM anther sections of wild-type (wt) Col-0 (**a, c, e, g, i**) and *ams* mutant (**b, d, f, h, j**). (**a, b**) TEM sections of pollen mother cells (PMC) pre-meiosis and tapetum in wt (**a**) and *ams* (**b**), showing normal tapetum (T) and PMC, middle layer (ML), Endodermis (En), Epidermis (Ep). Meiosis progresses normally in wt (**c, e**), whereas irregularities occur in the *ams* tapetum with pre-vacuolation (v) mutant tapetal cells (**d, f**). Connections between tapetum cells and PMC are seen in wt (**c, e**, arrows), whilst abnormal/compressed connections are seen in the *ams* mutant (**d, f**, arrows). Wild-type (**g**) showing callose cell wall deposition on developing meiocytes with cytokinesis occurring to form tetrads, while *ams* (**h**) has abnormal callose accumulation and separation. Normal tetrads are seen in wt (**i**) stage (Vacuoles: v), whereas abnormal tetrads and highly vacuolated (v) tapetum cells are observed in *ams* (**j**). Scale bar **c, d, g, h** = 5 μm, rest = 10 μm.

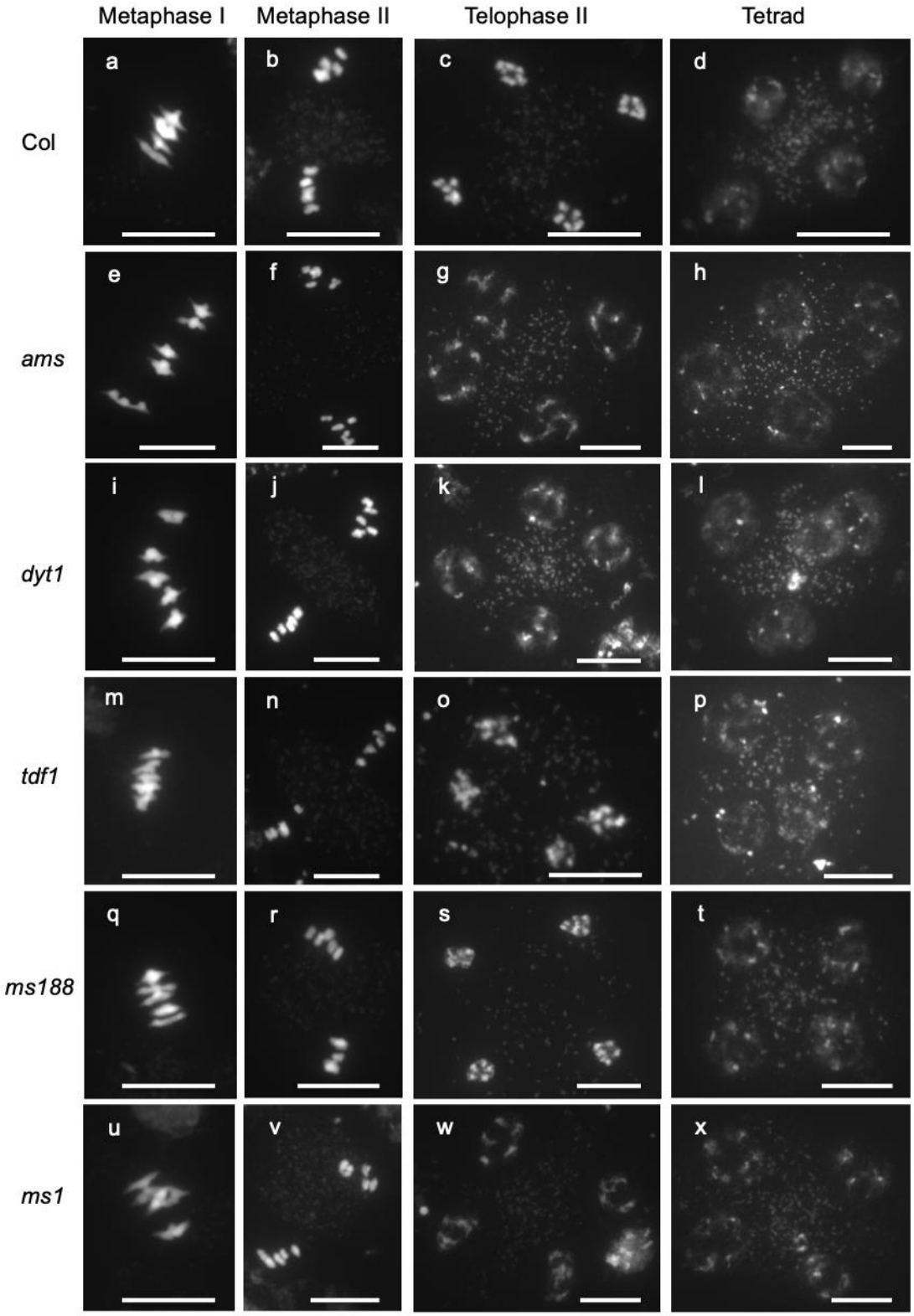

FIGURE 2. Male sterile mutants have normal early meiosis development.
4',6-Diamidino-2-phenylindole (DAPI) staining of wild-type (wt) and male sterile mutants *ams*, *dyt1*, *tdf1*, *ms188* and *ms1* meiocytes during male meiosis. The presence of five bivalents is clear at metaphase I and metaphase II in all lines, with correct separation occurring in metaphase II. During telophase II there is the balanced formation of four sets of five chromosomes with the correct formation of tetrads in all lines observed. Scale bar = 10μm.

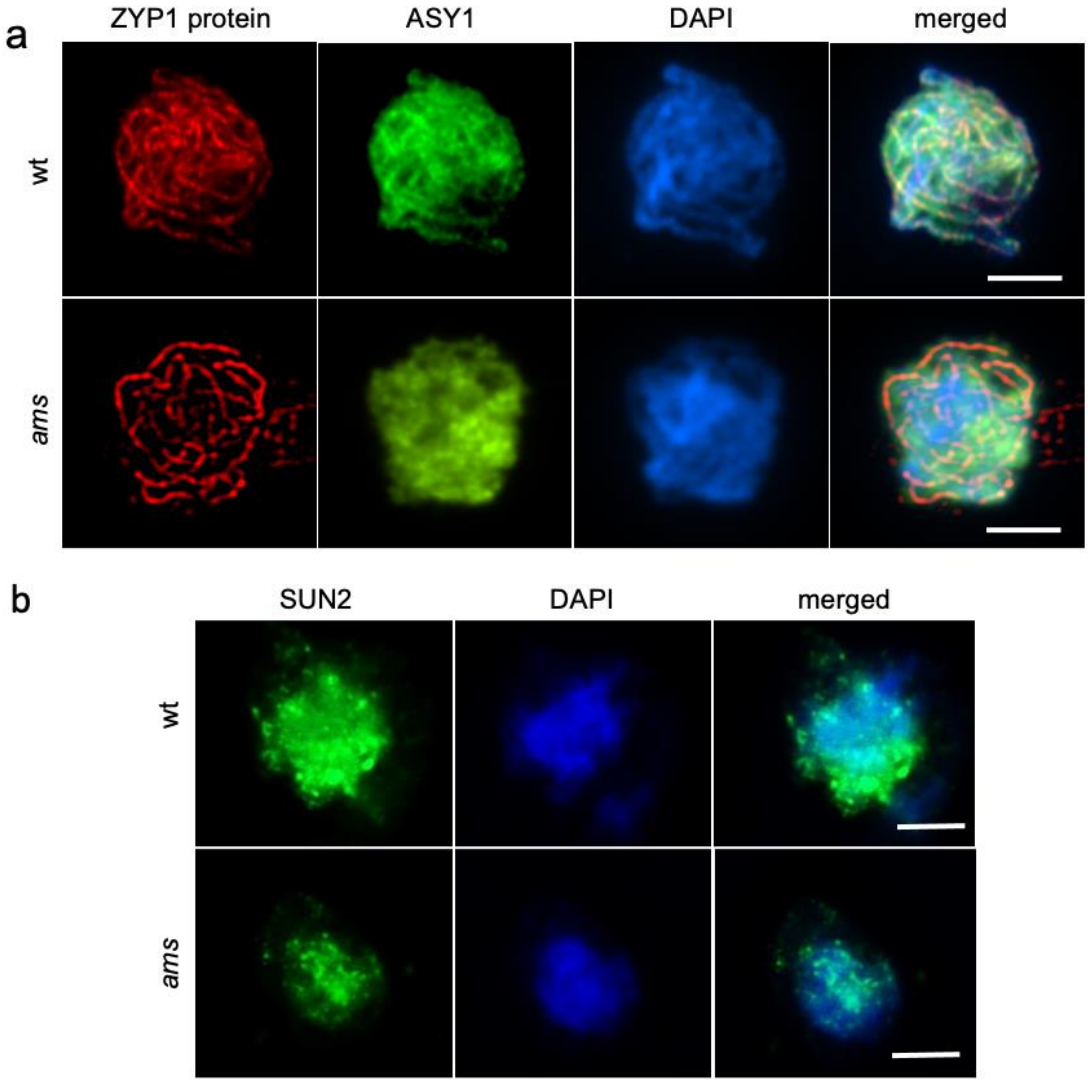

FIGURE 3. Chromosome pairing, synapsis and nuclear envelope formation appear normal in *ams*.

(a) Localisation of the synaptonemal complex protein ZYP1 (red) and the axis-associated protein ASY1 (green) at zygotene stage in wt and *ams*. The distribution of both proteins appears normal indicating that chromosome pairing and synapsis occur in the absence of AMS. Chromosomes are counterstained with DAPI (blue). Scale bar = 5 μm.

(b) Nucleoporin localisation in wt and *ams* pollen mother cells, similar nuclear envelope expression patterns of AtSUN2 in wild-type and *ams* at telophase II with AtSUN2 (green) antibody, counterstained using DAPI (blue), strongest SUN2 signal was observed in *ams*. Scale bars = 5μm.

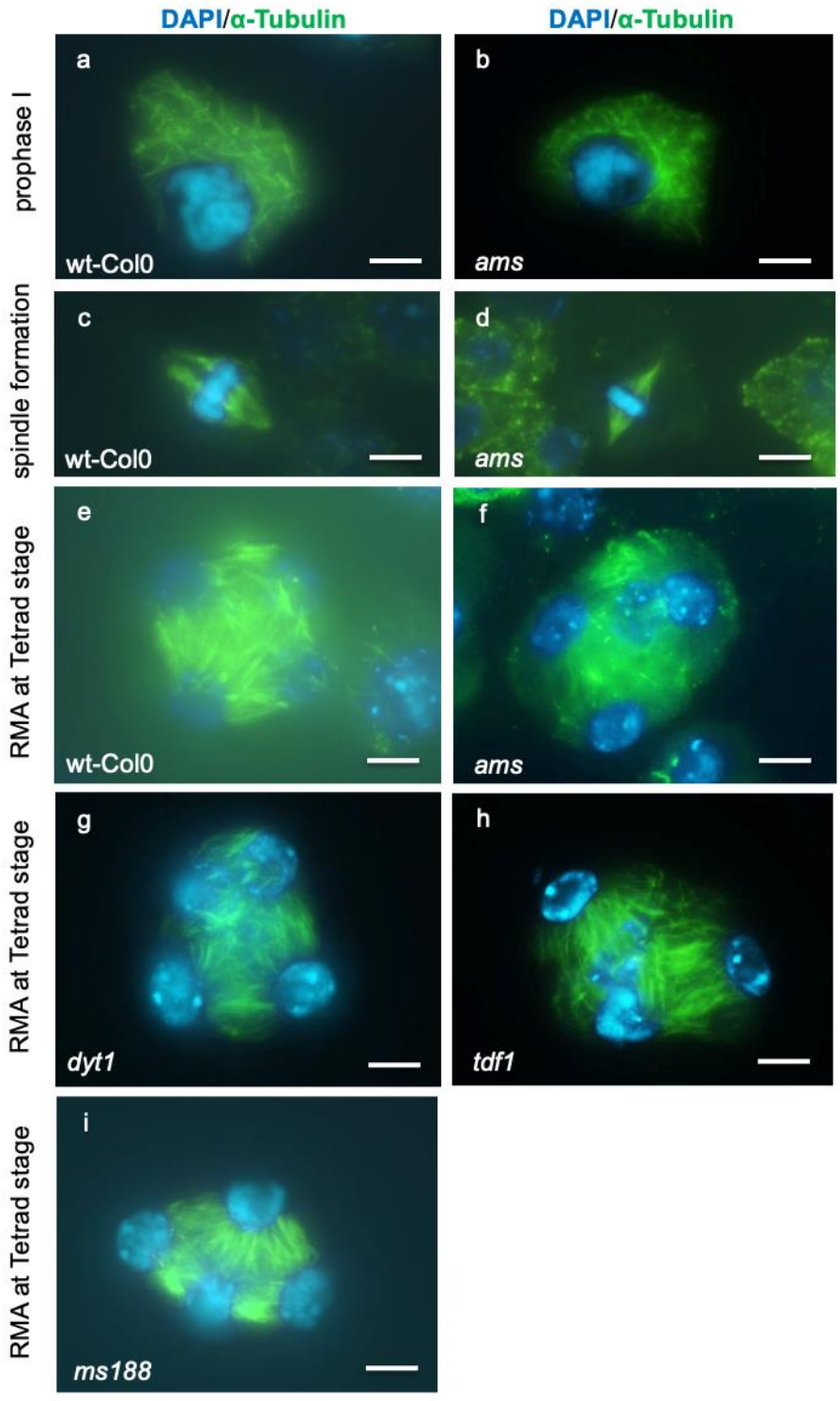

FIGURE 4. Spindle formation morphology in wild-type and male sterile meiocytes.
The spindle was detected by immunostaining with anti-α-tubulin antibody (green) and chromosomes were counterstained with DAPI (blue). Tubulin localisation is similar in wt Col-0 and *ams* at prophase I (a, b), with normal spindle morphology during metaphase I in Col-0 (c) and *ams* (d). Radial microtubule arrays (RMA) however are disorganised in *ams* (f) compared to wt (e), this is also observed in the upstream male sterile mutants *dyt1* (g), *tdf1* (h), but not the downstream mutant *ms188* (i). Nuclei positioning within the tetrad is also unbalanced forming a 'triad' like shape in *dyt1*, *tdf1*, and *ams* (g-i). Scale bar = 5μm.

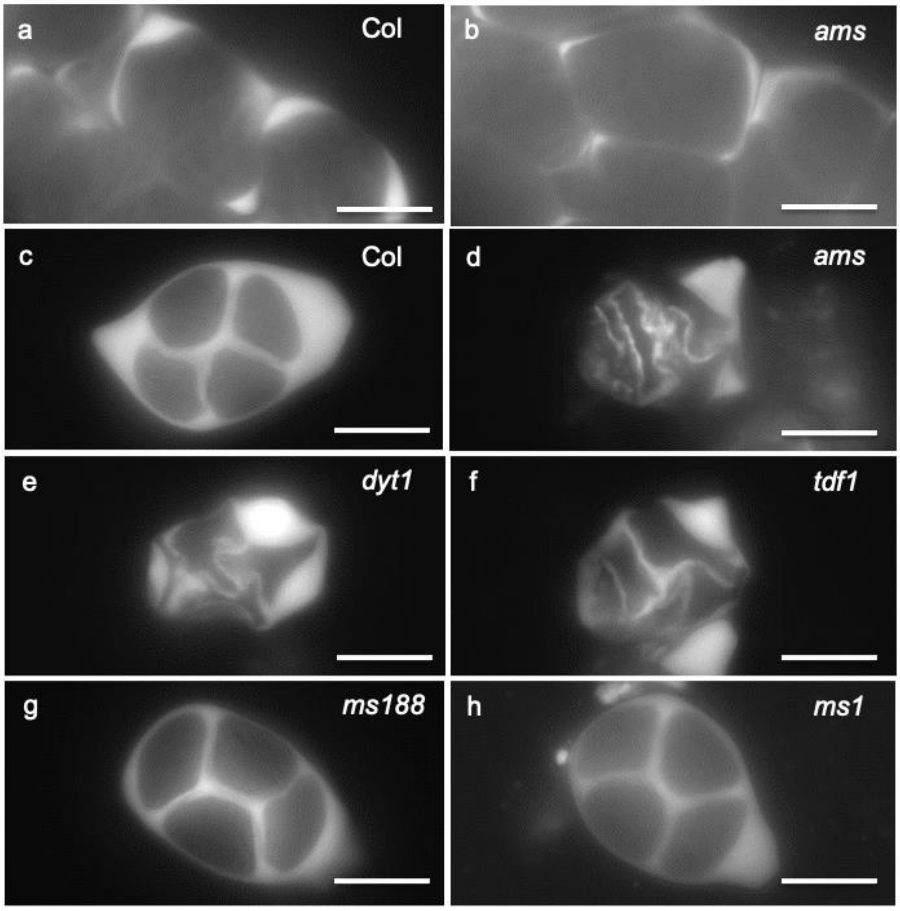

FIGURE 5. Callose staining of male meiocytes of tapetum defective mutants.

Callose staining of wild-type Col-0 (**a**) and *ams* (**b**) tetrads during meiosis initially showed similar callose production, suggesting normal initiation of callose biosynthesis. Callose deposition, forming thick walls surrounding the tetrads, was subsequently seen in wt **(c)**, whereas this was abnormal and disorganised in *ams* tetrads (**d**), *dyt1* (**e**) and *tdf1* mutants (**f**), whereas the later stage tapetum mutants, *ms188* (**g**) and *ms1* (**h**), showed normal callose deposition and thick, ordered callose layers surrounding the tetrads. Scale bars = 10 μm.

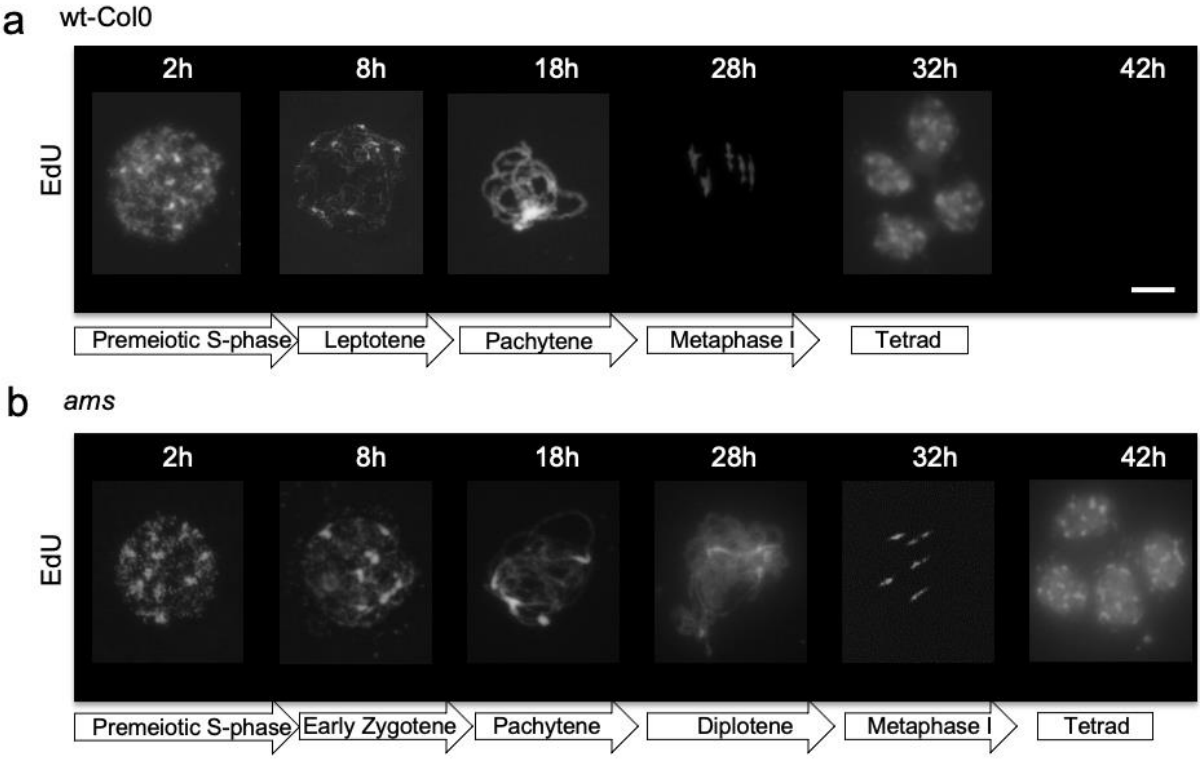

FIGURE 6. Meiotic progression over time in *ams* compared to wild-type.
Detection of EdU labelling in pollen mother cells across a time course of sampled cells (2h, 8h, 18h, 28h, 32h and 42h). EdU Alexa Fluor® 488 (white). (**a**) Wild-type Col-0 showing normal meiotic progression, with tetrads observed after 32h, whilst (**b**) *ams* showed delayed progression through meiosis after pachytene stage, with occasional tetrads observed only after 42h. Scale bar = 10μm.

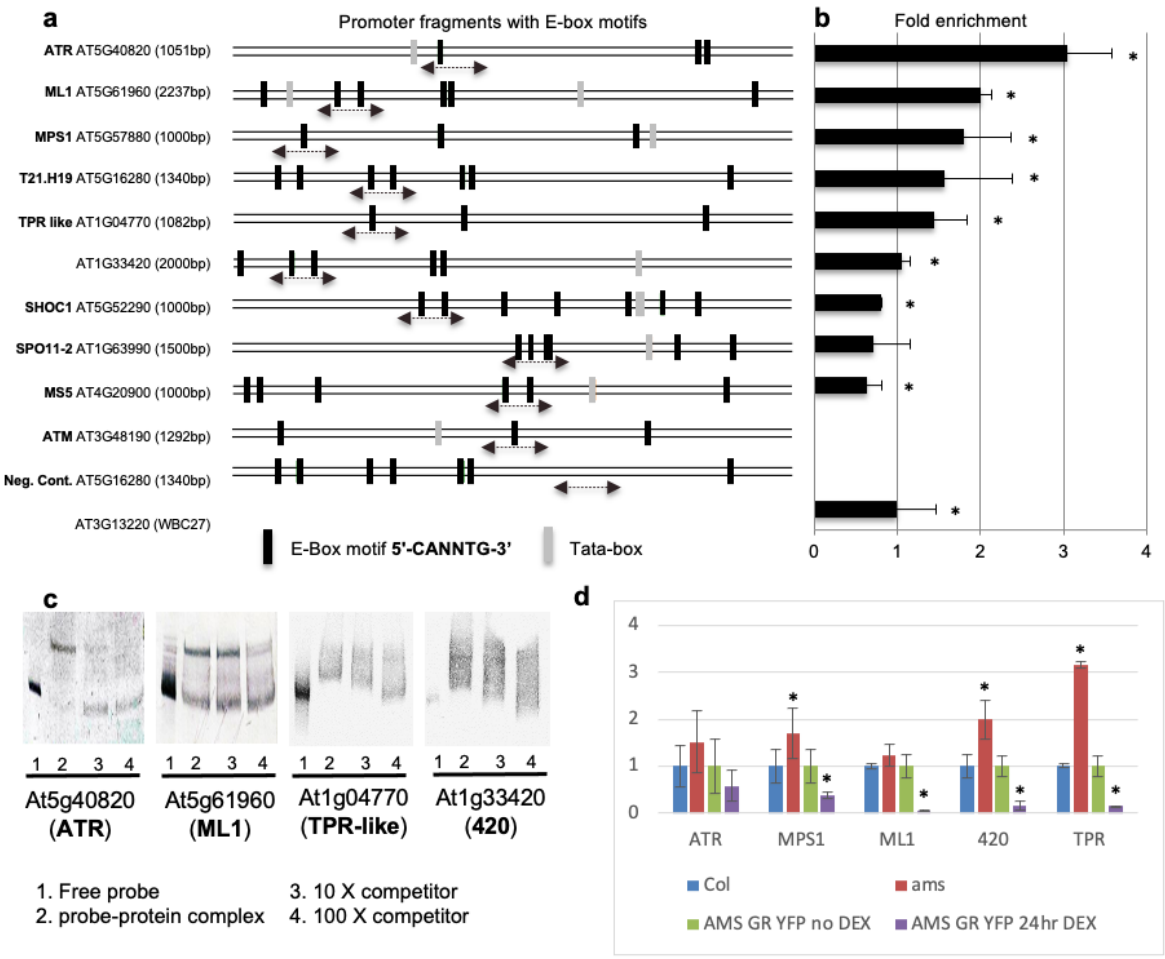

FIGURE 7. AMS binds directly to the promoters of selected meiotic-associated genes to regulate their expression.

(a) ChIP-qPCR analysis of the enrichment of AMS regulatory targets compared to WBC27 positive control. Predicted E-boxes in the promoter region represented by dark vertical lines and promoter regions analysed by ChIP-qPCR and EMSA represented by dotted line and arrows. (b) Fold enrichment represents the fold change in +Ab (antibody) compared with -Ab samples, normalised to WBC27 fold change. qPCR data were gathered from three biological and two technical replicates. Significant changes based on student t-test $P<0.05$ are represented by *. Error bar represent SD. (c) EMSA using digoxigenin (DIG) labelled probes without AMS protein or unlabelled probes (lane 1), lanes 2-4 show AMS protein and DIG labelled probe with increasing amount of competitor DNA (10x, 100x respectively). Gel retardation indicates the binding of the AMS to promoters of the target genes. (d) Relative expression values based on qRT-PCR analysis measured in whole inflorescence in wild-type (Col-0), *ams* and AMSprom:AMS-GR-YFP in wt Col-0 background. Showing up-regulation in *ams* mutant and down-regulated in the AMSprom:AMS-GR-YFP line 24 hours after AMS induction by DEX. Expression was normalised to wild-type (1) for *ams* and AMS-GR-YFP without DEX (1) for AMS-GR-YFP 24hr after DEX. Significant changes based on student t-test $P<0.05$ are represented by *. Error bars represent SE.

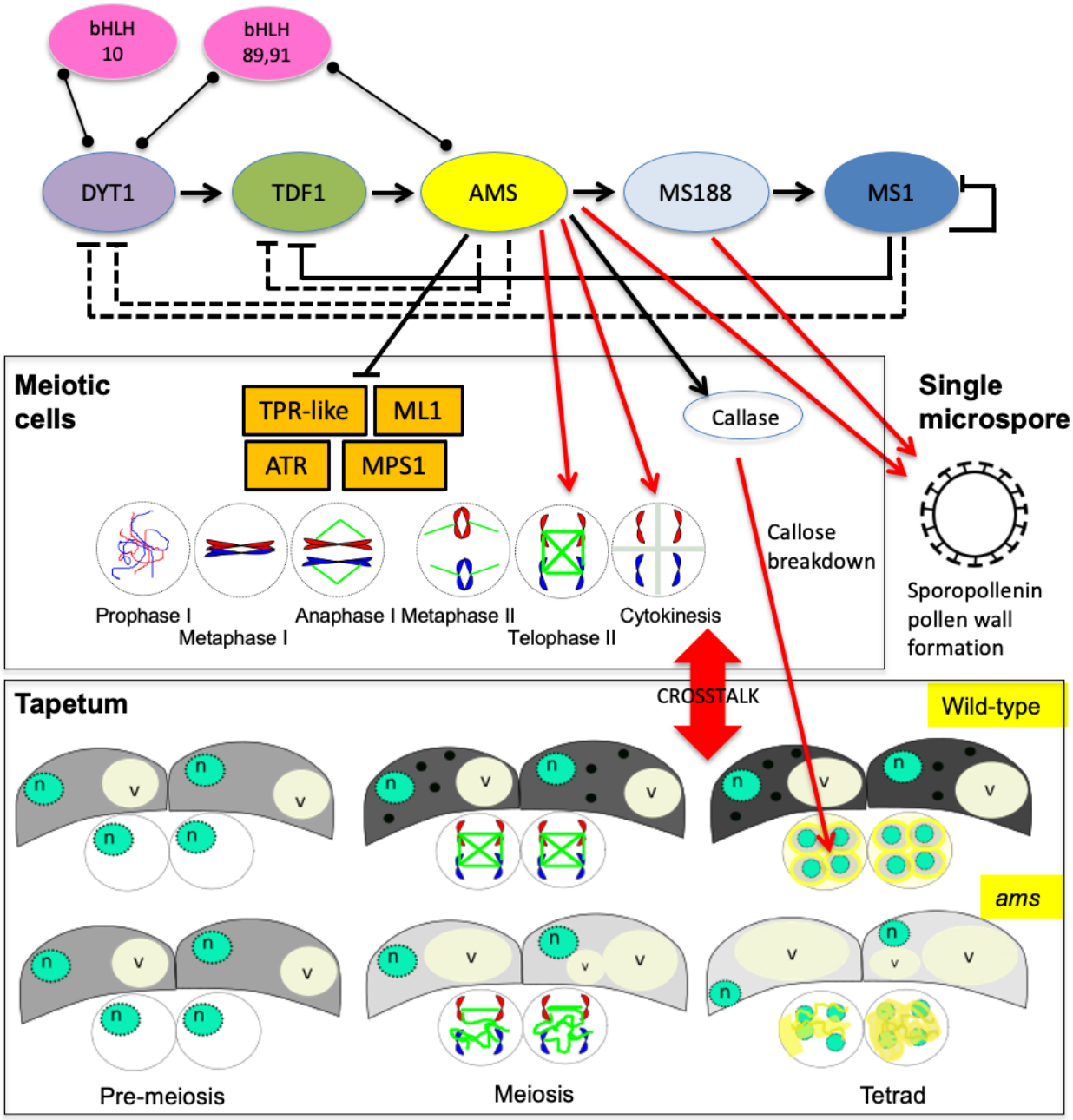

FIGURE 8. Proposed regulatory network for AMS.
Tapetum regulatory pathway based on network published in Ferguson et al., (2017), AMS is directly regulated by DYT1 through TDF1, and itself directly regulates MS188, which regulates MS1. AMS has a published role in sporopollenin wall formation alongside MS188. We propose that it is the loss of AMS in the early tapetum mutants that cause the phenotypes observed in *ams, tdf1* and *dyt1* mutants, as *ms188* and *ms1* develop normally. We have shown a novel role for AMS in the correct regulation of RMA localisation (green lines in meiocytes) during telophase II, for correct cytokinesis, callose wall deposition (yellow material in meiocyte) to produce a functional tetrad. AMS is also important for fully functional tapetum cells which have a high energy requirement during meiosis (darker background colour representing this, and black dots indicate lipidic tapetosomes and elaioplasts) to provide for the developing pollen. We have shown that AMS appears to directly negatively regulate at least 4 meiosis-associated genes, possibly through interaction in the tapetum, and propose that AMS has a role in the final stages of meiosis through their regulation. v: vacuole; n: nucleus. Arrows: regulation; lines ending with a line: repression; lines with a line ending with circle: protein interactions. Dashed lines indicate a minor role in regulation of network (as predicted by modelling (Ferguson et al. 2017)). Red lines indicate a major role in regulation.